N94- 35606

Modal Decomposition of Hamiltonian Variational Equations

William E. Wiesel
Department of Aeronautics and Astronautics
Air Force Institute of Technology
2950 P Street
Wright - Patterson AFB, Ohio 45433

Abstract

Over any finite arc of trajectory, the variational equations of a Hamiltonian system can be separated into "normal" modes. This transformation is canonical, and the Lyapunov exponents over the trajectory arc occur as positive / negative pairs for conjugate modes, while the modal vectors remain unit vectors. This decomposition effectively solves the variational equations for any canonical, linear time–dependent system. As an example, we study the Voyager I trajectory. In an interplanetary flyby, some of the modal variables increase by very large multiplicative factors, but this means that their conjugate modal variables decrease by those same very large multiplicative factors. Maneuver strategies for this case are explored, and the minimum Δv maneuver is found.

1 Introduction

A Hamiltonian dynamical system can be written as a vector set of differential equations

$$\dot{\mathbf{X}} = Z\frac{\partial H}{\partial \mathbf{X}}, \tag{1}$$

where $\mathbf{X}^T = (q_i,\ p_i)$ is termed the state vector, and the matrix Z is

$$Z = \begin{Bmatrix} 0 & I \\ -I & 0 \end{Bmatrix}. \tag{2}$$

Introduce the small displacement $\mathbf{x}(t) = \mathbf{X}(t) - \mathbf{X}_0(t)$ from a known trajectory $\mathbf{X}_0(t)$. Then, to first order in small quantities, the displacement vector obeys the variational equations

$$\dot{\mathbf{x}} = A(t)\mathbf{x} = Z\frac{\partial^2 H}{\partial \mathbf{X}^2}\bigg|_{\mathbf{X}_0}\mathbf{x}. \tag{3}$$

As a set of linear equations, the variational equations are formally solved by the fundamental matrix $\Phi(t, t_0)$, which satisfies

$$\dot{\Phi} = A(t)\Phi, \quad \Phi(t_0, t_0) = I. \tag{4}$$

Then, the general solution to (3) can be written as $\mathbf{x}(t) = \Phi(t, t_0)\mathbf{x}(t_0)$.

2 The Modal Transformation

In this section we will review the recent discovery of the modal transformation for general time dependent linear systems, Wiesel [6], and we will establish this transformation as a canonical change of coordinates.

The stability of a general trajectory of a linear system is determined by the Lyapunov exponents. These are the values

$$\lambda_i = \frac{1}{t_f - t_0} \log \frac{|\Phi(t_f, t_0)\mathbf{x}_i(t_0)|}{|\mathbf{x}_i(t_0)|}, \tag{5}$$

extremalized over all initial displacements $\mathbf{x}_i(t_0)$. Usually (5) includes a limit as $t_f \to \infty$, but not here. The restriction to finite time intervals is an absolute necessity, since prediction of chaotic systems is only possible for a finite time interval.

We wish to find the vectors $\mathbf{x}_i(t_0)$, which extremalize the growth of the norm of displacement vectors, $|\mathbf{x}(t_f)|$ with respect to the initial displacement $\mathbf{x}(t_0)$. This is a constrained maximization, since in a linear system we may specify $|\mathbf{x}(t_0)| = 1$ from the outset. Using a Lagrange multiplier μ, we have the optimization problem

$$J = |\mathbf{x}(t_f)|^2 - \mu \left(|\mathbf{x}(t_0)|^2 - 1 \right). \tag{6}$$

Now, since $\mathbf{x}(t_f) = \Phi(t_f, t_0)\mathbf{x}(t_0)$, the scalar function (6) becomes

$$J = \sum_i \left\{ \sum_j \Phi_{ij} x_{0j} \right\}^2 - \mu \left\{ \sum_i x_{0i}^2 - 1 \right\}. \tag{7}$$

Partial derivatives can now be calculated as if all components of the initial conditions x_{0i} were independent, yielding

$$\frac{1}{2}\frac{\partial J}{\partial x_{0k}} = 0 = \sum_i \sum_j \Phi_{ij}\Phi_{ik} x_{0j} - \mu_i x_{0k}, \tag{8}$$

where $k = 1, 2, ...N$. But this is just the component form of

$$\left\{ \Phi^T \Phi - \mu_i I \right\} \mathbf{e}_i(t_0) = 0. \tag{9}$$

That is, the $\mathbf{e}_i(t_0)$ are the real, orthogonal eigenvectors of the real symmetric matrix $\Phi^T\Phi$, or the right singular vectors of Φ. Comparison to (5) shows that the Lyapunov exponents over the time interval $(t_0,\ t_f)$ are found from

$$\mu_i = \exp\left\{ 2\lambda_i (t_f - t_0) \right\}. \tag{10}$$

This has been recognized by Goldhirsch, Sulem and Orszag [1]. We will refer to our λ_i as *regional* Lyapunov exponents, since they pertain to the finite time interval $(t_0,\ t_f)$.

A matrix Φ is symplectic if it obeys $\Phi Z \Phi^T = Z$, or equivalently $\Phi^T Z \Phi = Z$. It is well known that the fundamental matrix Φ is symplectic for a Hamiltonian dynamical system, see, e.g., Wiesel and Pohlen [7]. But then examining $\Phi^T\Phi$, we find

$$\begin{aligned} \Phi^T\Phi Z \left(\Phi^T\Phi\right)^T &= \Phi^T \left(\Phi Z \Phi^T\right) \Phi \\ &= \Phi^T Z \Phi = Z, \end{aligned} \tag{11}$$

so that $\Phi^T\Phi$ is itself symplectic. The eigenvalues of a symplectic matrix occur as inverse pairs, $\mu_i,\ 1/\mu_i$, so by (10) the regional Lyapunov exponents occur as positive / negative pairs. Since the Lyapunov exponents are also real, at most half of the modes are unstable, while the other half are stable. The proof of Liouville's theorem follows from this as a very simple consequence.

Over a finite arc of the trajectory, the regional Lyapunov exponents may be used to factor the dynamics into separate modes. The initial conditions $\mathbf{e}_i(t_0)$ introduce N special solutions to the variational equations, $\mathbf{x}_i(t) = \Phi(t, t_0)\mathbf{e}_i(t_0)$, on which the average exponential rate of expansion or contraction is an extremum. But local variations in these rates can be quite large, Haubs and Haken [2], Nese [3], Sepúlveda, Badii, and Pollak [4]. We wish to use these N special solutions to the variational equations as basis vectors for the entire solution set, and it would be very inconvenient for them to be anything other than unit vectors. Their instantaneous rates of change of magnitude are given by

$$\sigma_i(t) = \frac{\mathbf{x}_i \cdot A\mathbf{x}_i}{|\mathbf{x}_i|^2}. \tag{12}$$

Since the regional Lyapunov exponents are the average of these instantaneous rates on these N extremal solutions, we have

$$\lambda_i = \frac{1}{t_f - t_0} \int_{t_0}^{t_f} \sigma_i(\tau) d\tau. \tag{13}$$

Then, define N new functions $\mathbf{e}_i(t)$ as the solutions to

$$\dot{\mathbf{e}}_i(t) = A\mathbf{e}_i - \sigma_i(t)\mathbf{e}_i \tag{14}$$

with initial conditions $\mathbf{e}_i(t_0)$ on the interval (t_0, t_f). They are, by (14), trivially unit vectors on the entire interval $t_0 \leq t \leq t_f$, and orthonormal at $t = t_0$. That they must also be orthogonal at $t = t_f$ can be seen by realizing that $\mathbf{e}_i(t_f)$ must also be the extremal initial conditions for exponential growth of trajectories running *backwards* in time. So they are the eigenvectors of the symmetric matrix $(\Phi^{-1})^T(\Phi^{-1})$, and are orthogonal. But at other times in the interval (t_0, t_f) the $\mathbf{e}_i(t)$ vectors may not be orthogonal. We note that since the new vectors remain unit vectors,

$$\sigma_i(t) = \mathbf{e}_i \cdot A\mathbf{e}_i \tag{15}$$

is an alternate form of (12). The $\mathbf{e}_i$ have the same direction as the special solutions $\mathbf{x}_i$ throughout the time interval, differing from them only in magnitude.

Now, assemble the $\mathbf{e}_i(t)$ vectors by columns into the matrix $\mathcal{E}(t)$. The matrix analog of (14) is

$$\dot{\mathcal{E}} = A\mathcal{E} - \mathcal{E}J(t), \tag{16}$$

where $J(t)$ is the diagonal matrix whose entries are the $\sigma_i(t)$. This is a relationship which is very familiar from time–periodic systems.

We wish to use the $\mathbf{e}_i(t)$ vectors as the coordinate vectors for describing the solution to the variational equations. To this end, define new coordinates $\mathbf{y}$ on the tangent space as

$$\mathbf{x}(t) = \mathcal{E}(t)\mathbf{y}(t). \tag{17}$$

Since $\mathcal{E}(t)$ is a nonsingular matrix function of time, at least for $t_0 \leq t \leq t_f$, all stability information resides within the $\mathbf{y}$ variables. Again differentiating (17) and substituting into the variational equations (3) we have

$$\dot{\mathbf{y}} = \left\{\mathcal{E}^{-1}A\mathcal{E} - \mathcal{E}^{-1}\dot{\mathcal{E}}\right\}\mathbf{y}. \tag{18}$$

But using (16), this easily reduces to

$$\dot{\mathbf{y}} = J(t)\mathbf{y}. \tag{19}$$

So, this transformation takes the variational equations (3), and replaces them with a set of *decoupled, time–dependent coefficient* differential equations for the variables $\mathbf{y}$, and another set of linear equations (16) for the coordinate vectors $\mathbf{e}(t)$. We will refer to $\mathbf{y}$ as the *modal variables* for the system, and $\mathcal{E}(t)$ as the modal matrix.

The transformation (17) will be canonical if $\mathcal{E}$ is a symplectic matrix for all time. It is possible to so normalize $\mathcal{E}(t_o)$ at the initial time, Siegel and Moser [5], Wiesel and Pohlen [7]. Then $\mathcal{E}$ will stay symplectic if $\mathcal{E}^T Z \mathcal{E} = Z$ for all time. Taking a time derivative of this and substituting from (16) gives

$$\mathcal{E}^T A^T Z \mathcal{E} + \mathcal{E}^T Z A \mathcal{E} - J^T \left(\mathcal{E}^T Z \mathcal{E}\right) - \left(\mathcal{E}^T Z \mathcal{E}\right) J = 0. \tag{20}$$

Assuming that the modal matrix is at the moment symplectic replaces the quantities in parentheses with Z. For Hamiltonian systems the matrix $A = Z\partial^2 H/\partial X^2$, and since $\partial^2 H/\partial X^2$ is symmetric, the above reduces to

$$-J^T Z - ZJ = 0. \tag{21}$$

Simple calculation will show that this is an identity for any diagonal matrix J, so the modal transformation (17) is a canonical transformation if $\mathcal{E}(t_0)$ is symplectically normalized. The modal equations of motion (19) then come from a modal variational Hamiltonian

$$K(\mathbf{y}) = \frac{1}{2}\mathbf{y}^T Z^T J \mathbf{y}. \tag{22}$$

This is, of course, only a local approximation, ignoring cubic and higher order terms.

3 The Voyager 1 Trajectory

As an example, we have chosen to study an approximation to the Voyager I trajectory from earth past Jupiter, and onward almost to Saturn. The trajectory is only approximate, since it was constructed in the restricted problem of three bodies. But our method is general, and easily extends to more complex and realistic dynamics. The Hamiltonian function is

$$H = \frac{1}{2}\left(p_x^2 + p_y^2 + p_z^2\right) - p_x y + p_y x - \frac{1-\mu}{r_1} - \frac{\mu}{r_2}, \tag{23}$$

where

$$\begin{aligned} r_1^2 &= (x-\mu)^2 + y^2 + z^2, \\ r_2^2 &= (x+1-\mu)^2 + y^2 + z^2. \end{aligned} \tag{24}$$

Using Voyager I's known distance of closest approach to Jupiter of 780,000 km and the flight time of 544 days from the earth to Jupiter, a boundary value problem was posed: starting at Jupiter the trajectory was propagated backwards, and at "launch", it should be 1 A.U. from the sun, and moving tangentially. The initial conditions for this trajectory are listed in Table I. In addition, we give a point about 100 days prior to close approach.

Table I

Launch Initial Conditions

	x	y	z
q_i	$+3.762779457438691 \times 10^{-2}$	$+1.886728183030001 \times 10^{-1}$	0.0
p_i	$-2.991922520851858 \times 10^{0}$	$+5.825188979188912 \times 10^{-1}$	0.0

Intermediate Initial Conditions

	x	y	z
q_i	$-8.775683982224044 \times 10^{-1}$	$-4.272485353294678 \times 10^{-2}$	0.0
p_i	$-8.227825491293955 \times 10^{-1}$	$-7.044554120116425 \times 10^{-1}$	0.0

Over this trajectory, a final time of 1.5 dimensionless time units will take the spacecraft from the earth almost to the orbit of Saturn. This is shown in Fig. 1, in the rotating reference frame usually used for the restricted problem. The regional Lyapunov exponents are ± 5.637879, ± 5.08635, and ± 2.251739. Examining the eigenvectors, the first and third are modes in the orbital plane, while the second is purely an out of plane mode. This leads to amplification / contraction of initial errors by multiplicative factors of 4706, 2058, and 29.3. Over an infinite time interval we would expect two zero Lyapunov exponents, and the third mode is much the least dramatically unstable of the three. It probably corresponds to an initial displacement along the trajectory itself.

To gain further insight, adjacent trajectories have been examined in the modal space. Integrating the nominal trajectory and a nearby orbit, the difference $\mathbf{x} = \mathbf{X}(t) - \mathbf{X}_0(t)$ was converted into modal variables with $\mathbf{y} = \mathcal{E}^{-1}\mathbf{x}$. Initial conditions were chosen to excite only one mode at a time, and to explore the limit of the linearization inherent in our solution. A shorter arc of the trajectory, spanning ± 100 days before and after flyby was chosen in order to avoid the extreme differences between initial and final modal amplitudes. Initial conditions for this arc are also given in Table I, and the limits of this portion of the trajectory are indicated in Fig. 1. Over this interval, the first two modes expand/decay by a factor of about 400, while the third mode is nearly static with an expansion/contraction factor of 1.32. The corresponding Lyapunov exponents are ± 20.213590, ± 20.161805, ± 0.935968. The study of a shorter, less violently expanding / contracting interval makes it possible to see the entire modal behavior on graphs. It also emphasizes that neither the Lyapunov exponents nor the modal vectors $\mathcal{E}$ are invariant to changes in the trajectory arc studied.

Fig. 2 shows the behavior of the Lyapunov exponents through this time interval. That is, the figure plots the running values of $\lambda_i(t)$ starting 100 days before Jupiter approach, and ending 100 days afterwards. The final values are the Lyapunov exponents used to decouple the entire trajectory arc, but intermediate values show where error growth occurs. Obviously, the immediate vicinity of the close approach is a time of explosive error growth. But after the flyby some of this error growth decays again.

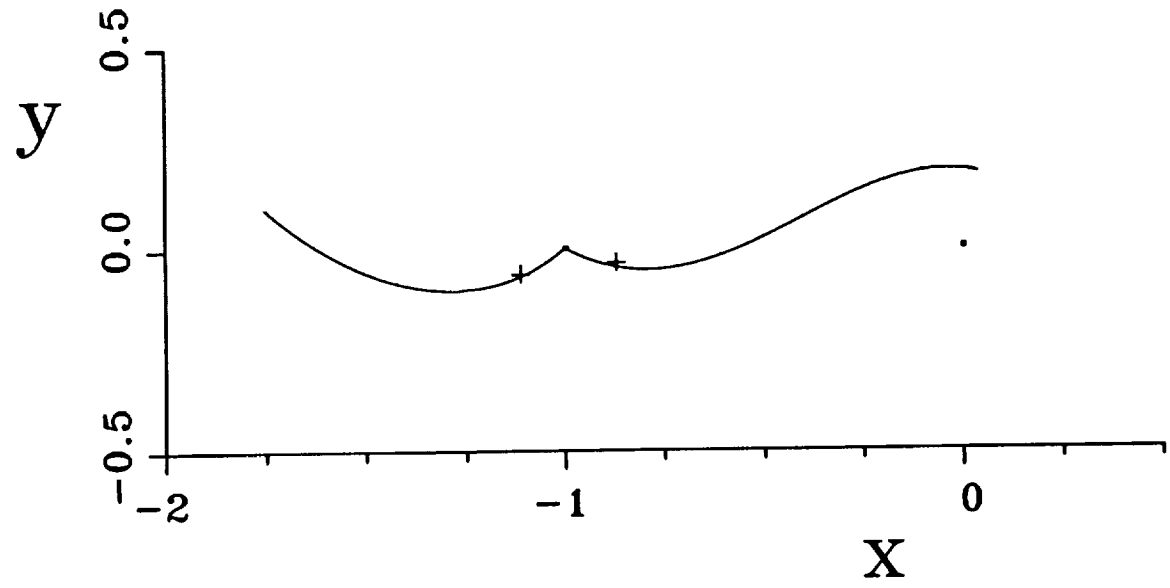

Figure 1: Voyager I flyby trajectory in the rotating frame of the restricted problem. Jupiter is at the cusp, while plus signs mark points ±100 days bracketing close approach.

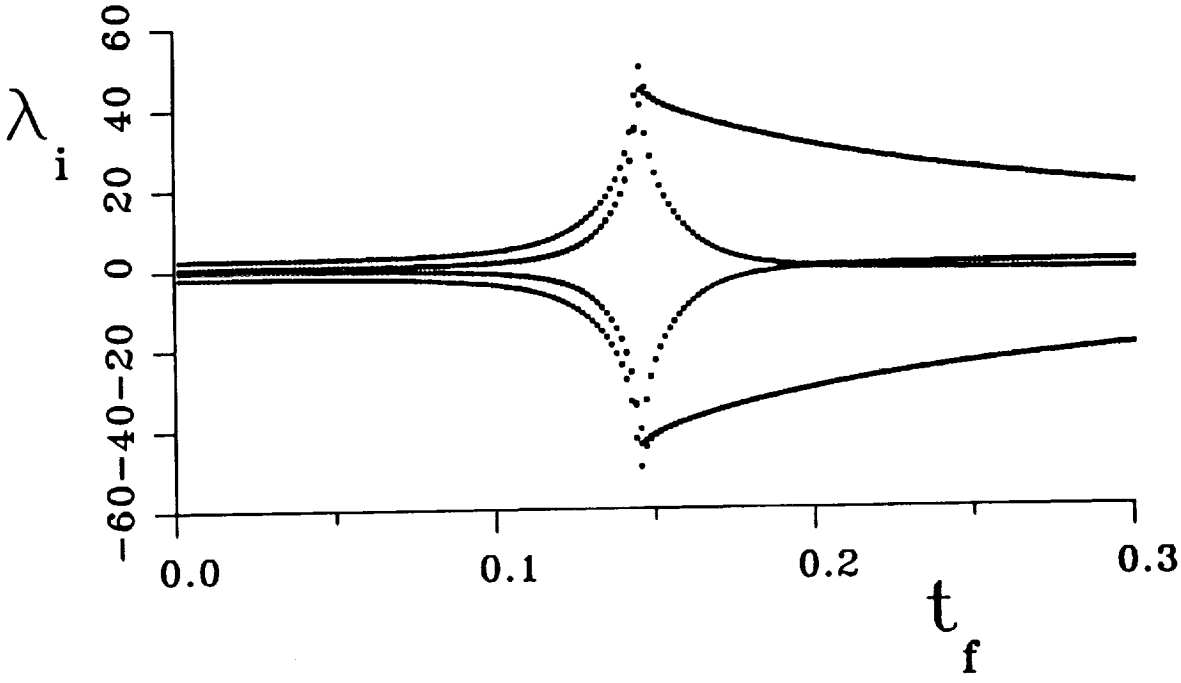

Figure 2: Lyapunov exponents $\lambda_i(t_f)$ throughout the ±100 day interval bracketing flyby. The first and second modes (the outer curves after flyby) are superimposed at this scale.

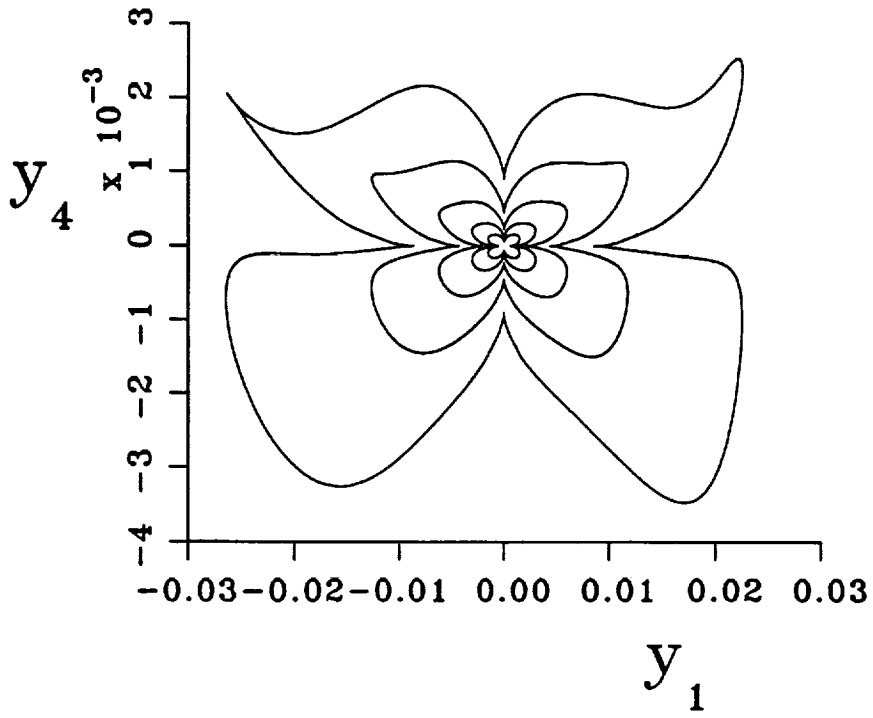

Figure 3: Modal trajectories on the tangent space for mode 1, with Lyapunov exponents ± 20.21359.

Fig. 3 shows the behavior of the first mode over the ± 100 day arc. The modal vectors for this mode lie entirely within the orbital plane of Jupiter. Since the modal equations of motion (19) are time dependent, Fig. 3 is not a true phase portrait. Rather, initial conditions were scaled by a constant factor to find where the system visibly departs from linearity. Since y_1 grows by a factor of about 400 in this interval, while y_4 shrinks by the same factor, initial conditions are virtually on the vertical y_4 axis, while all trajectories terminate nearly on the horizontal y_1 axis. The linear regime appears at the core of the figure as a symmetric region where trajectories scale linearly. Most of the loop is traversed in a *very* short period of time about closest approach. Over most of the time interval trajectories are slowly departing from the vicinity of the y_4 axis before flyby, or converging towards the y_1 axis after closest approach. These trajectories were calculated with initial values of y_2, y_3, y_5, and y_6 zero. These values stayed zero, confirming the success of the modal transformation.

Fig. 4 shows tangent space trajectories for the second mode. This mode lies entirely along the z, p_z directions in phase space, and the error growth / shrinkage factor is again about 400 over this trajectory arc. The truly linear regime again appears at the core of the figure, while the outer trajectories show visible departures from linearity. Also like mode 1, virtually all of the outer loops are traversed in a short time interval bracketing closest approach.

Mode 3 appears to span the in-track direction and the normal vector to the constant Hamiltonian surface. Since errors in these two directions are, in the long run, nearly static, the author suspects that if extended to infinity that this mode would generate the predicted pair of zero Lyapunov exponents. (A pair since in any autonomous system one Lyapunov exponent must be zero, and as a canonical system its Lyapunov exponents must occur as positive / negative pairs.) Fig. 5 shows some trajectories for this mode. The expansion / contraction of amplitude near close approach is so dramatic for this mode that all the initial and final points for this mode are at the origin on this scale plot. Actual initial modal amplitudes were of the order of 10^{-7}, and expand briefly by over four orders of magnitude near close approach. The individual trajectories seem to leave the origin, and then virtually retrace their outward path in returning.

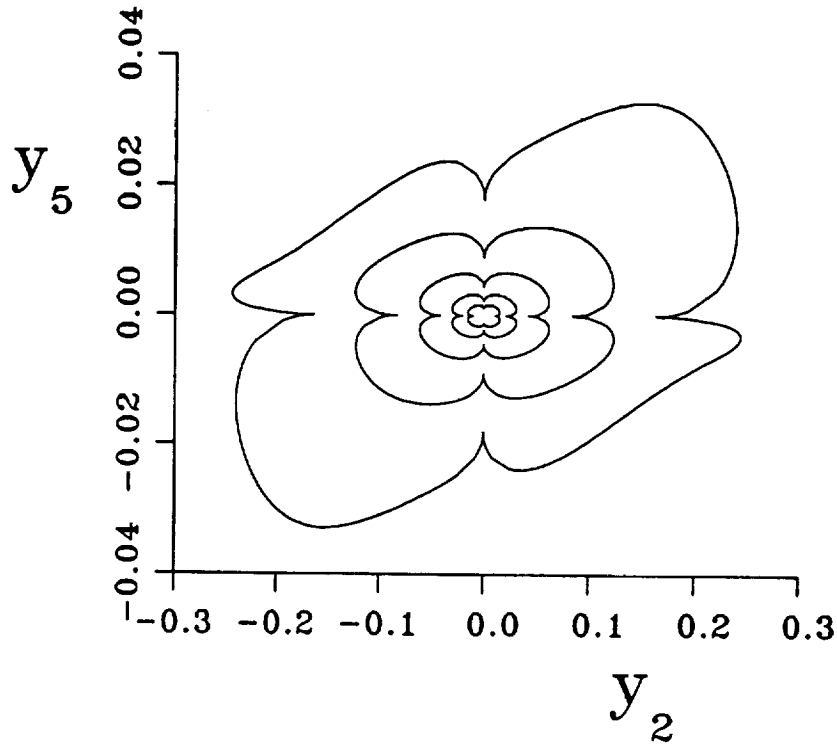

Figure 4: Tangent space trajectories for mode 2, the out-of-plane mode. The Lyapunov exponents are ±20.16180.

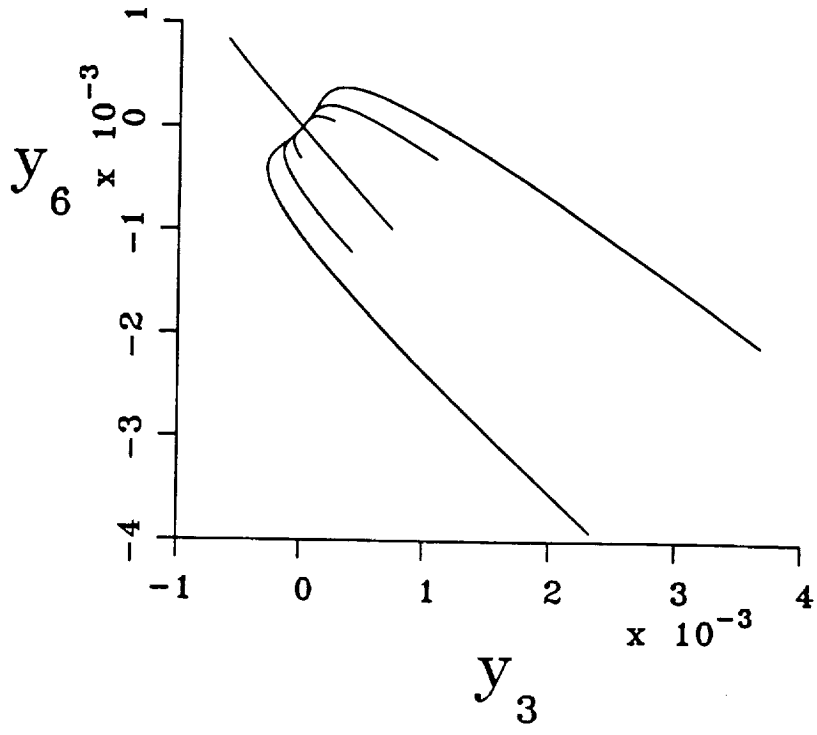

Figure 5: Tangent space trajectories for the third mode, with Lyapunov exponent ±0.93596. At this scale, all trajectories begin at and return to the origin.

4 Maneuvers

Since three Lyapunov exponents are positive, while three are negative, we have examined a maneuver strategy which attempts to zero the unstable modal amplitudes y_1, y_2, y_3. The stable modal amplitudes are far less important, since they are decreasing any ways. However, we can only perform impulsive changes in velocity in the physical space, and we have just stated our maneuver goals in the modal space. Just before a maneuver, we have

$$\mathbf{x}(t^-) = \mathcal{E}(t)\mathbf{y}(t^-), \tag{25}$$

while just afterwards we have

$$\mathbf{x}(t^-) + \delta\mathbf{x} = \mathcal{E}(t)\mathbf{y}(t^-) + \mathcal{E}\delta\mathbf{y}. \tag{26}$$

Subtracting the two equations above produces $\delta\mathbf{x} = \mathcal{E}\delta\mathbf{y}$. Now, physically we must have $\delta\mathbf{x}^T = (0^T,\ \delta\mathbf{v}^T)$, since an impulsive maneuver cannot change the position vector, and since the momenta are really the components of the inertial velocity on the rotating frame axes. In partitioned form, then, the maneuver conditions become

$$\begin{pmatrix} 0 \\ \delta\mathbf{v} \end{pmatrix} = \begin{Bmatrix} \mathcal{E}_{11} & \mathcal{E}_{12} \\ \mathcal{E}_{21} & \mathcal{E}_{22} \end{Bmatrix} \begin{pmatrix} \delta\mathbf{y}_{1-3} \\ \delta\mathbf{y}_{4-6} \end{pmatrix}, \tag{27}$$

in three by three vector partitions. To zero the unstable modal amplitudes we must have

$$\delta\mathbf{y}_{1-3}^T = (-y_1,\ -y_2,\ -y_3). \tag{28}$$

The changes in the stable modal amplitudes are not within our control. The first three rows can be solved to yield

$$\delta\mathbf{y}_{4-6} = \mathcal{E}_{12}^{-1}\mathcal{E}_{11} \begin{pmatrix} -y_1 \\ -y_2 \\ -y_3 \end{pmatrix}. \tag{29}$$

Then, the second three rows give the desired maneuver as

$$\delta\mathbf{v} = \left\{\mathcal{E}_{21} + \mathcal{E}_{22}\mathcal{E}_{12}^{-1}\mathcal{E}_{11}\right\} \begin{pmatrix} -y_1 \\ -y_2 \\ -y_3 \end{pmatrix}. \tag{30}$$

An alternate strategy is suggested by the fact that only two of the modes experience significant expansion, while mode three is nearly static. Attempting to zero only the amplitudes of modes one and two enables us to minimize the velocity change required in the maneuver. Rewrite (27) as

$$\begin{pmatrix} \delta\mathbf{y}_{1-3} \\ \delta\mathbf{y}_{4-6} \end{pmatrix} = \begin{Bmatrix} \mathcal{E}_{11}^{-1} & \mathcal{E}_{12}^{-1} \\ \mathcal{E}_{21}^{-1} & \mathcal{E}_{22}^{-1} \end{Bmatrix} \begin{pmatrix} 0 \\ \delta\mathbf{v} \end{pmatrix}. \tag{31}$$

(The $\mathcal{E}_{ij}^{-1}$ are three by three blocks of the inverse matrix $\mathcal{E}^{-1}$.) Then, we wish to minimize Δv^2 subject to the constraints $\epsilon_1\Delta\mathbf{v} = -y_1$ and $\epsilon_2\Delta\mathbf{v} = -y_2$, where the ϵ_i are the first and second rows of $\mathcal{E}_{12}^{-1}$. Using two Lagrange multipliers λ_i, the minimum amplitude maneuver is given by the solution to the five linear equations

$$\begin{aligned} &2\Delta v_i + \lambda_1\epsilon_{1i} + \lambda_2\epsilon_{2i} = 0,\ \ i = 1,2,3\,, \\ &\epsilon_1\Delta\mathbf{v} = -y_1, \\ &\epsilon_2\Delta\mathbf{v} = -y_2. \end{aligned} \tag{32}$$

To study this maneuver strategy, we have begun at 100 days before flyby with a unit error in either y_1 or y_2. Of course, this is a linear problem, and scales linearly to other initial errors. Then the error was corrected at maneuver time t_m, and the new state, including nonzero amplitudes in the modal variables y_{4-6}, was propagated to 100 days after the flyby. The results for y_1 are shown in Figs. 6 and 7. Fig. 6 shows the required Δv maneuver amplitude as a function of the maneuver time in order to eliminate a unit error in y_1 at the start of the trajectory arc. As expected, the error is much cheaper to correct early in the trajectory, and becomes very expensive to correct after flyby. Fig. 7 shows the final values $y_{4-6}(t_f)$ as a function of the

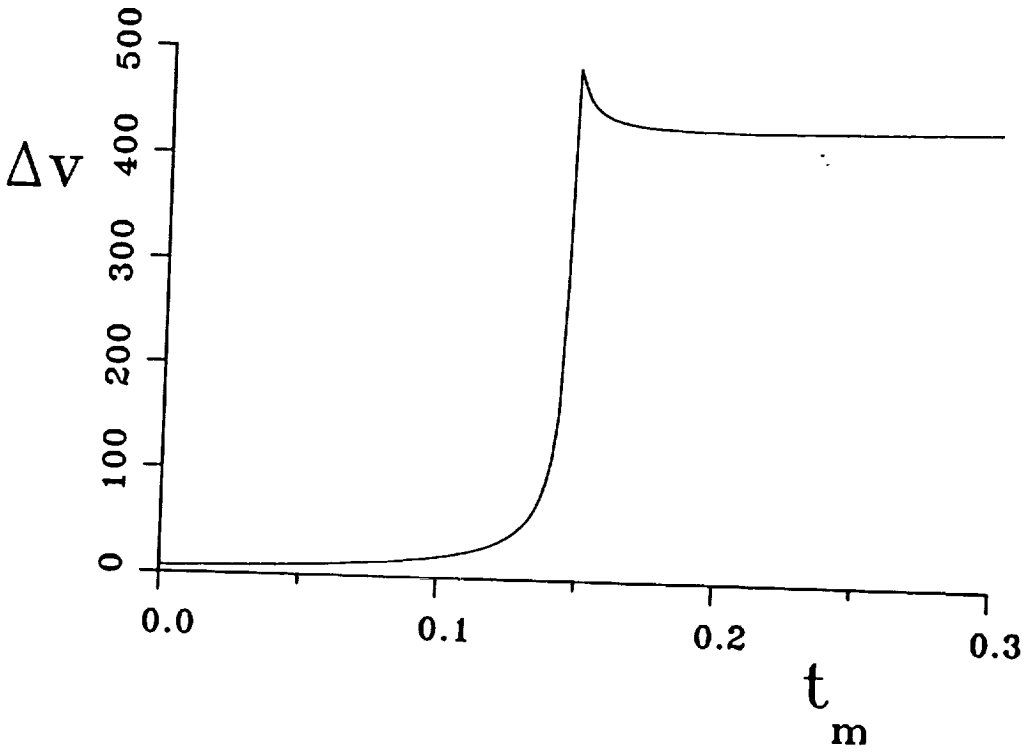

Figure 6: Maneuver magnitude Δv needed to correct an initial unit error in y_1 as a function of the time of the maneuver t_m. The error is vastly cheaper to correct before flyby.

time at which the maneuver is performed. Both y_3 and y_6 suffer a very large unwanted increase (again, at the final time) if the initial y_1 error is corrected any time around close approach. The conjugate variable to y_1, y_4, remains insensitive to y_1 corrections before close approach, since any error introduced into y_4 by an early maneuver has considerable time in which to decay. This is not true after the flyby, and the final error $y_4(t_f)$ shows a linear growth with t_m for maneuvers performed after the time of closest approach. The out of plane mode y_5 is decoupled from the planar modes, so it remains at its initial value of zero.

Figs. 8 and 9 show the analogous results for an initial unit error in the unstable vertical mode y_2. The cost of correcting an out of plane error soars enormously just at the time of closest approach, and afterwards drops to a lower, nearly static value. The nearly static cost afterwards is due to the fact that most of the mode growth / contraction in this problem occurs very near the time of flyby. Afterwards most of the modal amplitudes themselves become almost static. Fig. 9 shows the final modal amplitudes as a function of the maneuver time. Since the z mode is decoupled from both planar modes, these are not excited from their initial zero values. However, the stable mode y_5 conjugate to the unstable vertical mode y_2 is excited by maneuvers performed after the close approach. As with the planar mode, this is due to the fact that y_5 can significantly decay if the maneuver is performed before the flyby, but does not greatly decay if the maneuver is performed after flyby.

5 Discussion and Conclusions

In this paper we have shown that the recently discovered modal separation for time dependent linear systems can be put on a canonical footing. A numerical example has been presented, showing the modal behavior and maneuver strategies for an approximation to the Voyager I flyby of Jupiter. The modal separation variables make it possible to assess the effects of initial errors and the steps taken to correct them without reference to the actual size of the errors, and making maximum use of the possible dynamical decoupling that the modal transformation offers.

This is just a beginning. There is no reason that the orbit determination process itself could not use the modal variables as the quantities to be determined. Also, the fact that the modal transformation is itself

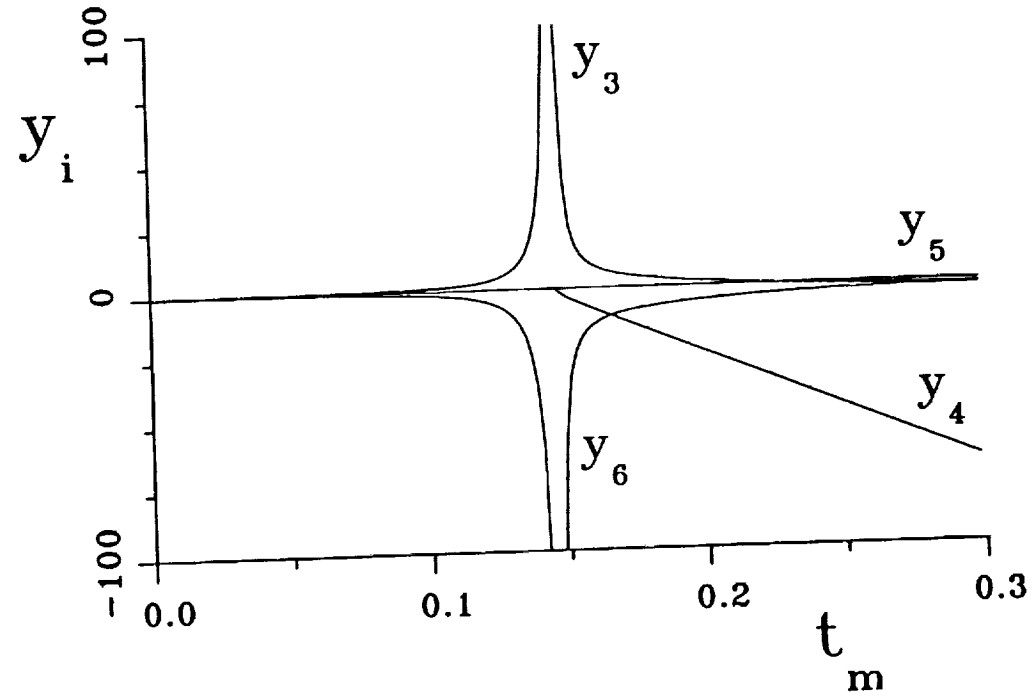

Figure 7: Final modal amplitudes $y_i(t_f)$ as a function of the time t_m a maneuver was performed to cancel an initial unit error in y_1.

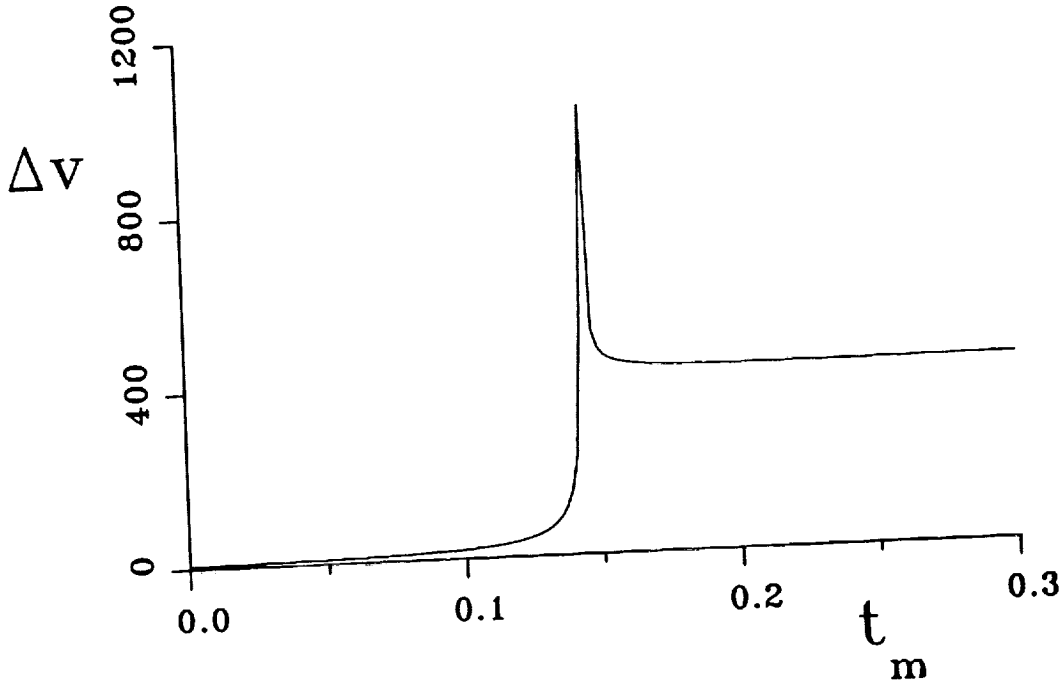

Figure 8: Maneuver cost Δv needed to cancel an initial unit error in the out of plane mode y_2.

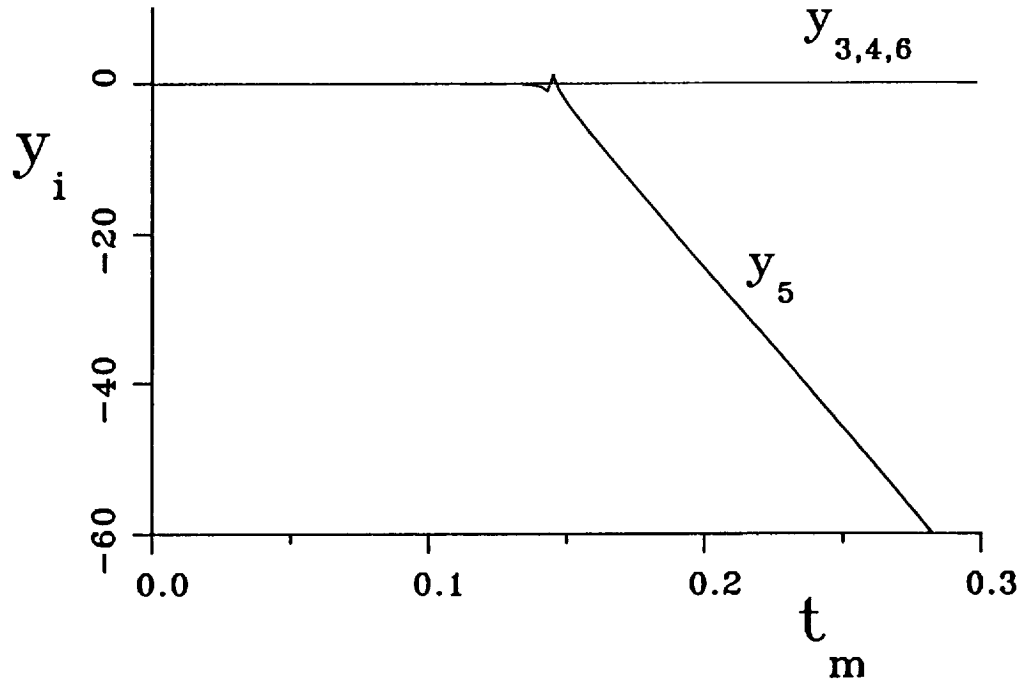

Figure 9: Final modal amplitudes $y_i(t_f)$ as a function of the maneuver time t_m used to correct an initial unit error in the unstable vertical mode y_2.

a canonical transformation might be used to construct a *perturbation theory* about the underlying reference orbit, including higher order terms in the modal Hamiltonian (22) as the perturbation source. This might significantly extend the region of validity of the linearization of the trajectory.

References

[1] I. Goldhirsch, P.-L. Sulem, and S.A. Orszag: 1987. *Physica D*, **27**, pp. 311-337.

[2] G. Haubs and H. Haken: 1985. *Z. Phys. B*, **59**, pp. 459-468.

[3] J.M. Nese: 1989. *Physica D*, **35**, pp. 237-250.

[4] M.A. Sepúlveda, R. Badii, and E. Pollak: 1989. *Phys. Rev. Lett.*, **63**, pp. 1226-1229.

[5] C.L. Siegel and J.K. Moser: 1971. "Lectures on Celestial Mechanics", *Springer–Verlag*, New York, pp 100-103.

[6] W. E. Wiesel: 1994. *Phys. Rev. E.* to appear, March 1994.

[7] W. E. Wiesel and D. J. Pohlen: 1994. *Celest. Mech and Dynamical Astronomy*, **58**, 81–96, 1994.